Control-Oriented Modeling of Wet Clutch Friction considering Thermal Dynamics

Seungin Shin[a], Seibum B. Choi[b,*]

[a]Samsung Electronics, 1, Samsung-ro, Giheung-gu, Yongin-si, Gyeonggi-do, 17113, Republic of Korea
[b]Department of Mechanical Engineering, KAIST, 291 Daehak-ro Yuseong-gu, Daejeon, 34141, Republic of Korea

ARTICLE INFO

Keywords:
vehicle powertrain
wet clutch
friction model
friction coefficient
model-based control

ABSTRACT

The paper presents a control-oriented modeling method for wet clutch friction, considering thermal dynamics, with a focus on paper-based friction linings. Abrupt engagements of such clutches may lead to discomfort and reduce the overall lifespan. The limitations of feedback control, attributed to restricted sensors and modeling inaccuracies, underscore the effectiveness of model-based control employing precise and invertible models. The study extensively explores the largest model uncertainty in slip control—clutch friction. The proposed model integrates the Coulomb friction coefficient, incorporating variables such as pressing force, friction speed, and the temperature of the friction surface. The proposed torque model enables model inversion, allowing the determination of desired oil pressure from torque requirements. Experimental data, comprising 184 sets, validate the model accuracy, with a focus on temperature effects. The Coulomb friction coefficient model exhibits exponential and linear components, capturing the Stribeck effect and temperature variations. Model verification through experiments demonstrates good agreement, supporting its efficacy for wet clutch control performance. The study contributes insights into wet clutch friction models for model-based control.

1. Introduction

The clutch system serves to connect and disconnect two rotating shafts. It finds application in engines, transmissions, and differentials in vehicles, where clutches are frequently engaged and disengaged during driving. In vehicles, dry clutches are employed for manual transmission (MT), dual-clutch transmission (DCT), and automated manual transmission (AMT), while wet clutches are utilized for automatic transmission (AT), continuously variable transmission (CVT), and limited-slip differentials (LSD). Due to their superior heat resistance, wet clutches are preferred in transmissions for high-performance vehicles or heavy passenger cars requiring high torque capacity. An abrupt engagement of the clutch may result in an engagement jerk, causing inconvenience to the driver, and repeated incorrect engagements can also reduce the clutch's lifespan. The gear shift in an AT is achieved through clutch-to-clutch shifts, and model-based automatic control can enhance ride comfort by mitigating shifting jerks [1, 2].

In the field of automatic control, feedback (FB) control acquire more attention than feedforward (FF) control. However, the practical impact on control result may vary. In the case of AT, achieving satisfactory slip control through FB is challenging due to the rapid gear shift, limited sensors, and the inherent nonlinearity of the system. Consequently, control techniques actively incorporating precise and invertible models prove more effective. Therefore, model-based control utilizing the inverse of the system model becomes a suitable choice. Techniques such as the two degree-of-freedom (2-DOF) controller, feedback linearization, sliding mode control, and backstepping control are frequently employed in controlling nonlinear systems [3]. The 2-DOF controller is particularly apt when a precise system model is available, as in this study [4].

The largest model uncertainty in slip control of wet clutches arises from clutch friction. After Coulomb [5] proposed the concept of the friction coefficient, a dominant factor in the clutch engagement process, research results show that it is affected by various variables such as the pressing force, the temperature of the friction surface, and the friction speed. Numerous studies, including those using finite element methods (FEM), have focused on modeling clutch friction. For instance, Berger et al. [6] considered film dynamics with factors like applied load, friction material permeability, and radial groove dimensions. Other studies explored tribological modeling, incorporating hydrodynamic pressure, heat transfer, and film thickness dynamics [7]. Clutch torque modeling studies considered film thickness dynamics, friction lining permeability, and interface temperature [8]. Holgerson and Lundberg [9, 10] investigated the transition of engagement behavior concerning drive torque and changes in static and kinetic friction coefficients at different initial temperatures. Contact and wear characteristics of a typical paper-based friction materials were made by observation using contact microscopy [11].

Existing research has mainly focused on two friction materials: paper-based materials [7, 9, 10, 12, 13, 14, 15] generally used in AT clutches and a brass materials [16, 17, 18, 19, 20] used in limited-slip differentials. The friction and wear characteristics of these two kinds of friction materials under dry conditions were investigated [21]. This study specifically addresses paper-based friction lining. Automatic

*Corresponding author
si0.shin@samsung.com (S. Shin); sbchoi@kaist.ac.kr (S.B. Choi)
ORCID(s): 0000-0002-2859-0757 (S. Shin); 0000-0002-8555-4429 (S.B. Choi)

transmission fluid (ATF) satisfying the SAE 75W standard serves as coolant, lubrication, and piston pressure oil in ATs (see SAEJ311 for more information).

Control-oriented modeling of wet clutch systems requires lumped element models and static maps for straightforward friction calculations. Prior studies have explored control-oriented modeling of friction coefficients for brass and dry friction materials [22, 23]. Notably, the study by Wu et al. [24] analyzed the integrated friction coefficient, considering pressing force, friction speed, and oil temperature for paper-based friction materials. However, the study analyzed the integrated friction coefficient in which viscous friction was not separated in the friction coefficient calculation and used the oil temperature as a variable, not the friction surface temperature. Research on the anti-shudder property [20], and a study on constructing a heat transfer model for the same experimental set-up [16] have been conducted. There was a fundamental study on the friction coefficient using a simplified pin-on-disk experiment [17]. Ivanović et al. [18, 19] studied the transition of the friction coefficient and a method of estimating the surface temperature using the heat transfer equation, and they developed a model that simulates the parameters of the actual clutch system using a lumped-parameter model.

Another significant element of modeling for FF control is model inversion. The solution for most control problems is finding the control input for achieving the desired reference value. In FF control, the inverse function of the model is often used to calculate the desired system input.

Friction coefficient static maps assume variation based on the current value of each variables, while dynamic models consider variables' differentials, such as the change in pressing force. Each has its advantages and disadvantages, with dynamic models often requiring more characteristic values and extensive research on the target clutch, but the results are in good agreement with the model and experimental results. Static maps, while simpler, may not fit certain conditions; nevertheless, they have shown efficacy at high-pressure changes and speeds [25].

Research has sought to enhance automatic transmission control by applying friction coefficient models. Temperature-induced changes in the Coulomb friction coefficient, if left uncompensated, can significantly reduce control performance [20]. Efforts to extend clutch life have also been explored by analyzing clutch friction characteristics [2]. They used a simple qualitative technique of ramping down the pressure on the clutch at a specific time to achieve a smooth engagement and prevent excessive clutch temperature increase. However, in order to obtain satisfactory control performance, a more systematic and quantitative approach than simple techniques was required for the friction model considering temperature dynamics.

This study aims to contribute to the limited body of knowledge on wet clutch friction models usable for model-based control, particularly for paper-based friction linings considering temperature effects. The proposed friction model enables model inversion using a reduced-order model and a static map for control-oriented modeling. Based on the experimental data, a friction model considering the friction surface temperature for clutches with paper-based friction lining material was proposed and validated through experiments. Notably, the Coulomb friction coefficient depends on the temperature of the friction surface, and estimating this temperature involves considering heat transfer dynamics.

This paper is written with the following structure. Section 2 first describes the reduced-order models used in the study, including thermal dynamics, oil film thickness, and the clutch torque model. Section 3 details the design and configuration of the experimental equipment, the sensors used, the experiment for modeling, the results, and the development of the control-oriented friction modeling method based on these results. Section 4 presents a gear shift control example employing the proposed clutch torque and friction model. Finally, Section 5 concludes the paper.

2. Modeling

Prior to modeling the clutch friction torque, the automatic transmission system and gear shifting process will be explained to establish assumptions. The AT is a sophisticated system comprising a torque converter, planetary gear sets, clutches (brakes), pistons, and variable force solenoids (VFS). Combinations of clutches determine the gear ratio of the planetary gear sets, and the torque generated from the engine and torque converter is transmitted to the output shaft through the gear sets. Figure 1 illustrates the reduced-order schematic graph during the shift from the first to the second gear in an 8-speed automatic transmission. This gear shift involves two planetary gear sets and two brakes in the planet carrier and the second sun gear. Each engagement of the brakes corresponds to the first and second gears. In the figure and model, planetary gear sets, shafts, and clutches not involved in shifting from the first to the second are omitted and compressed into a single equivalent inertia and gear ratio γ_{in}. The reduced-order system comprises a total of 5 DOF: engine and torque converter pump I_E, torque converter turbine and front part of planetary gear sets I_{eq0}, brake 1 I_{eq1}, brake 2 I_{eq2} and vehicle mass I_V. If only the rear part of the torque converter is considered, it has 3 DOF. The transmission and tire have separate DOF due to a compliance model representing the torsion of the drive shaft that connects them.

The wet multi-plate clutch system operates with a hydraulic actuator, and the cross-section schematic diagram is depicted in the Fig. 2. Working fluid from the VFS enters the pressure chamber, pushing the piston to bring the multi-plate clutches into contact, resulting in friction. The higher the pressure in the chamber, the more the piston compresses the clutches, generating a greater friction torque. A simplified schematic diagram is drawn in Fig. 3. When pressure is relieved in the pressure chamber, the spring returns the piston to its original position. The inner and outer shafts are illustrated, and the role of the clutch is to transmit torque between the two shafts.

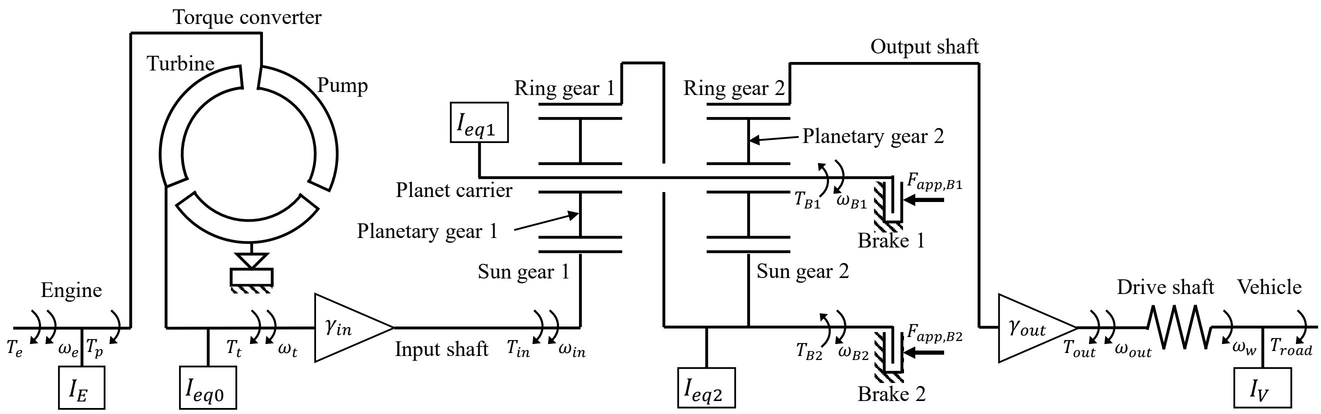

Figure 1: Schematic diagram of shifting from 1st to 2nd gear of an automatic transmission.

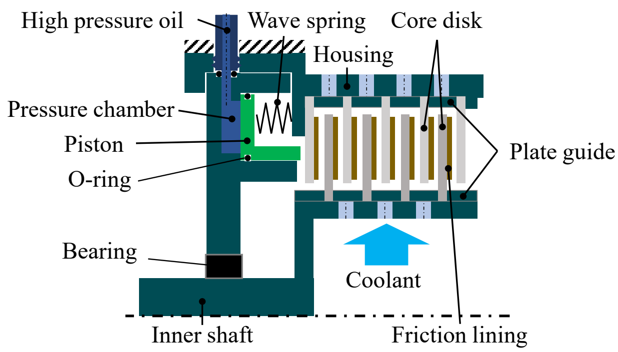

Figure 2: Schematic diagram of a multi-plate clutch (brake) system.

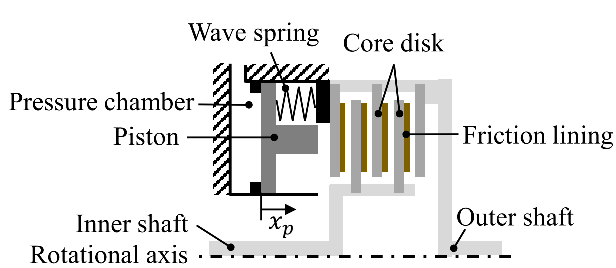

Figure 3: Simplified schematic diagram of a multi-plate clutch (brake) system.

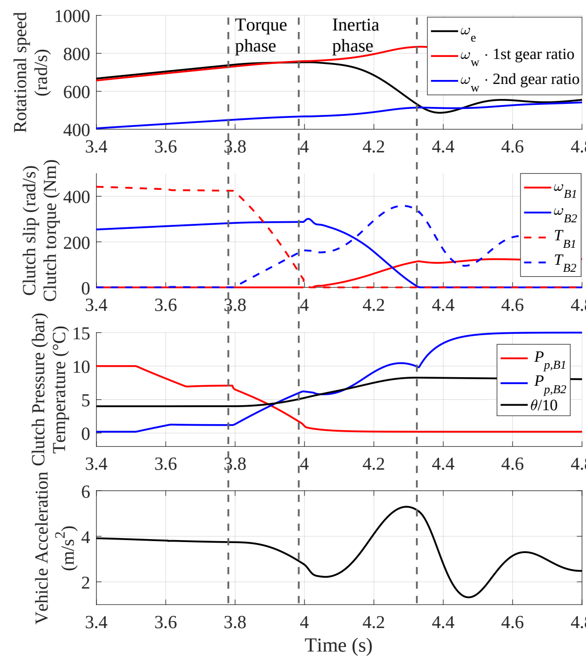

Figure 4: Graphs of major variables in a typical gear up-shift.

2.1. Gear shift procedure

A graph depicting the major variables in a typical gear up-shift is presented in Fig. 4. The clutch-to-clutch gear shift generally comprises two phases: a torque phase that transfers the torque from the clutch engaged in the previous gear to the clutch responsible for the next gear, and an inertia phase that smoothly engages the clutch by adjusting the engine speed through precise control of engine torque and clutch torque. In the torque phase, the off-going clutch finally loses all pressure and does not participate in the inertia phase (i.e., $T_{B1} = 0$). Precise control is required for the on-coming clutch, necessitating accurate and continuous pressure control to ensure smooth gear shifting in the inertia phase. When shifting gears in a heavy vehicle with a powerful engine, the clutch generates significant heat, causing a rise in the temperature of the friction surface. As temperature is a major variable affecting the Coulomb friction coefficient, it should be considered in control strategies.

Smooth shifting is attained by precisely managing the on-coming clutch pressure during the inertia phase. Since the on-coming clutch is already pressurized in the torque phase before entering the inertia phase, it can be assumed that the oil film dynamics in the inertia phase are at a steady-state. The simplified film thickness model using the steady-state assumption is discussed in detail in section 2.5.

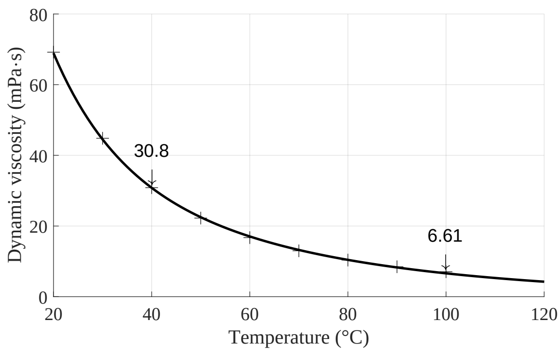

Figure 5: Dynamic viscosity μ_v of ATF.

2.2. Thermal dynamics

Using FEM for real-time surface temperature estimation is not preferred in control-oriented modeling. Straightforward models are necessary for such purposes. The heat balance equation is effective in estimating the clutch friction surface temperature within an acceptable margin of error. Given that the clutch separator and core disk are typically constructed from thin steel, known for its excellent heat conductivity, assuming a uniform temperature distribution in the separator is reasonable. In the case of a single-sided clutch, it can be further assumed that the separator and lining share the same temperature [8]. Consequently, treating the entire clutch pack as a lumped mass with a uniform temperature distribution is a valid approximation.

The zero-dimentional heat balance equation for the clutch pack can be written as:

$$\{(mc_p)_{lining} + (mc_p)_{separator}\} N_c \dot{\theta} \\ = T\Delta\omega - k_1(\theta - \theta_{oil}) - k_2(\theta - \theta_{housing}), \quad (1)$$

where m and c_p are the mass and specific heat capacity of the friction lining and separator plate, T is the wet clutch torque, $\Delta\omega$ is a slip speed of a clutch, k_1 and k_2 are the generalized thermal conductivity of convection from the clutch pack to the cooling oil and conduction to the housing, respectively. The term θ, θ_{oil} and $\theta_{housing}$ are the temperature of the clutch pack, oil reservoir and the temperature of the structures in direct contact with the clutches. In general, the two temperatures are the same in an actual transmission, but in this research, they differed due to structural limitations and were measured for analysis. The thermal conductivity k_1 and k_2 were identified experimentally in the next section.

For more accurate temperature estimation of the clutch system, see: detailed modeling considering the heat transfer and fluid hydrodynamics of an AT multi-disk wet clutch [8]; clutch temperature estimation using the heat transfer model of an automated manual transmission (AMT) of a heavy-duty truck [26].

2.3. Dynamic viscosity

The dynamic viscosity μ_v of ATF is a function of temperature. Its value is denoted by + and was fitted as the sum of two exponential functions as shown in Fig. 5. The specific values vary from manufacturer to manufacturer.

$$\mu_v(\theta) = \mu_{v1} e^{\mu_{v2}\theta} + \mu_{v3} e^{\mu_{v4}\theta}, \quad (2)$$

where μ_{v1} to μ_{v4} are dynamic viscosity parameters.

2.4. Clutch torque model

The effective radius and mean slip speed of the clutch are given by:

$$R_{eff} = \frac{2}{3}\frac{R_o^3 - R_i^3}{R_o^2 - R_i^2}, \quad (3)$$

$$v = R_{eff}\Delta\omega, \quad (4)$$

where R_{eff} is a torque effective radius of the clutch, R_o and R_i are the outer and inner radii of the clutch disk, and $\Delta\omega$ is the clutch rotational slip speed. Wet clutch torque T consists of Coulomb friction torque T_c and viscous torque T_v:

$$T = T_c + T_v, \quad (5)$$

$$T_c(v, \theta, F_c) = R_{eff} N_c \mu_f(v, \theta) F_c, \quad (6)$$

$$T_v(v, \theta, \bar{h}) = R_{eff} N_c \mu_v(\theta) A_f \frac{v}{\bar{h}}, \quad (7)$$

where θ is the mean temperature of the friction surfaces of the clutches, N_c is the number of friction pairs, μ_f and μ_v are the Coulomb friction coefficient and dynamic viscosity of the oil respectively, F_c is the normal force, A_f is the nominal contact area of the lining material, and $\bar{h}$ is the average fluid film thickness. From (5, 6, 7), we have

$$T(v, \theta, F_c, \bar{h}) = R_{eff} N_c \big(\mu_f(v, \theta) F_c \\ + \mu_v(\theta) A_f \frac{v}{\bar{h}}\big). \quad (8)$$

2.5. Film thickness model

For Gaussian distribution of asperity heights, the average fluid film thickness $\bar{h}$ has the following relation [27] with the nominal separation of the clutches h:

$$\bar{h} = \frac{h}{2}\left[1 + \mathrm{erf}\left(\frac{h}{\sqrt{2}\sigma}\right)\right] + \frac{\sigma}{\sqrt{2\pi}} e^{-\left(\frac{h}{\sqrt{2}\sigma}\right)^2}. \quad (9)$$

The normal force applied to the clutches F_{app} consists of two parts: the reaction force caused by the deformation of the friction lining material F_c, and the hydrodynamic force that squeezes out the fluid between the clutches F_h.

$$F_{app} = F_c + F_h = \iint_{A_f} p_c dA_f + \iint_{A_f} p_h dA_f. \quad (10)$$

where p_c is an asperity pressure and p_h is a hydrodynamic pressure.

The mean asperity pressure is given by the ratio of the real contact area A_c to A_f [28]:

$$p_c = E\frac{A_c}{A_f}, \tag{11}$$

where E is Young's modulus of the friction lining material. According to Greenwood and Williamson [29], A_c for Gaussian distribution of asperity heights is calculated as

$$A_c = \pi N A_f \beta\sigma F_1(\frac{h}{\sigma}), \tag{12}$$

$$F_n\left(\frac{h}{\sigma}\right) = \frac{1}{\sqrt{2\pi}}\int_{\frac{h}{\sigma}}^{\infty}\left(s-\frac{h}{\sigma}\right)^n e^{-\frac{1}{2}s^2}ds, \tag{13}$$

where N, β, and σ is, respectively, asperity density, asperity tip radius, and RMS roughness. For $n = 1$,

$$\begin{aligned} F_1\left(\frac{h}{\sigma}\right) &= \frac{1}{\sqrt{2\pi}}\int_{\frac{h}{\sigma}}^{\infty}\left(s-\frac{h}{\sigma}\right)e^{-\frac{1}{2}s^2}ds \\ &= \frac{1}{\sqrt{2\pi}}\left[e^{-\left(\frac{h}{\sqrt{2}\sigma}\right)^2} - \frac{h}{\sigma}\sqrt{\frac{\pi}{2}}\operatorname{erfc}\left(\frac{h}{\sqrt{2}\sigma}\right)\right], \end{aligned} \tag{14}$$

where erfc means complementary error function. From (11, 12, 14), we get

$$p_c(h) = \sqrt{\frac{\pi}{2}}EN\beta\sigma\left[e^{-\left(\frac{h}{\sqrt{2}\sigma}\right)^2} - \frac{h}{\sigma}\sqrt{\frac{\pi}{2}}\operatorname{erfc}\left(\frac{h}{\sqrt{2}\sigma}\right)\right]. \tag{15}$$

Many studies dealing with oil film dynamics show that the equivalent first-order system has a time constant of 0.05 to 0.1 s. As mentioned, when a steady-state such as the inertia phase of the gear shift is reached, the reaction force by the fluid pressure is zero, and the mean asperity pressure p_c causes the only reaction force. Then (10) becomes,

$$F_{app} = \iint_{A_f} p_c dA_f = p_c A_f = F_c. \tag{16}$$

Now we can calculate the average film thickness $\bar{h}$ from the measured force F_{app} of the load cell (6 of Fig 7.) by (15) and (16). It is useful to use pre-calculated array data of the (15) and interpolate it to get the inverse value, $\bar{h}(p_c)$, of the equation which is a monotonic function.

For control-oriented modeling, the system output should be a function of the system input. In a clutch system, oil pressure and clutch torque are inputs and outputs. Clutch friction torque consists of Coulomb friction and viscous friction. Each can be calculated with the proposed reduced-order model, and finally, the clutch torque that is the sum of the two can be obtained. Another thing to consider is that the model is a monotonic function, so model inversion is possible, so the desired oil pressure can be obtained from the desired torque.

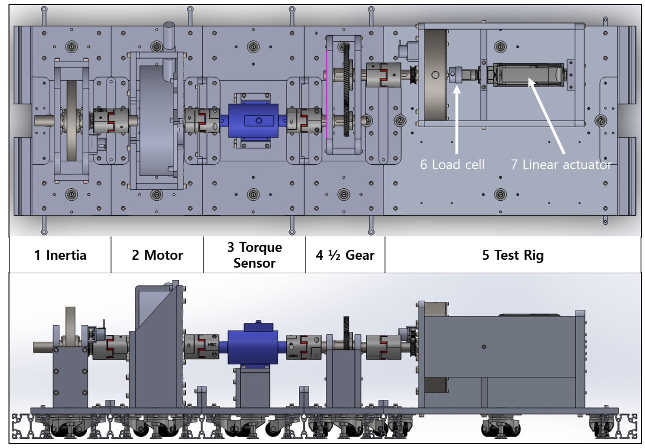

Figure 6: Overview of the test bench.

3. Experimental work

3.1. Experimental environment

As illustrated in Fig. 6, the experimental equipment mainly consists of motor 2, torque sensor 3, test rig 5, load cell 6, and linear actuator 7. The motor controls the rotational speed of the entire rotating body, including the inertia 1, so the desired speed is maintained. In this study, we used a hybrid vehicle motor with a maximum power of 32 kW and a maximum torque of 120 Nm. To get the desired rotational speed, the torque capacity of the motor and the motor controller need to cover the clutch torque range to be tested.

The motor torque passes through the gear 4, a torque amplifier, and reaches the clutches 14 and 15, where the braking torque by the linear actuator takes place. The cross-section of the test rig is illustrated in Fig. 7: a rotary encoder 8 that measures the rotational speed of the input shaft 10; a piston 9 that transmits the pressing force of the linear actuator; an outer guide 11, which is coupled to the outer-toothed clutches 15 and fixed to the housing and an inner-guide 12, which is coupled with the inner-toothed clutches 14 and fixed with the input shaft; and protection plates 13 and 16 are presented. Inner and outer guides were machined to give the clutches a DOF along the axial direction. Oil flows into the rig through an inlet, passes between the gaps and the clutch grooves, cools the clutch, and exits through the outlet to reach the reservoir. As the outlet is higher than the inlet, the rig is filled with oil.

Actual photos of the clutch are shown in Fig. 8. Their radii and thicknesses are given in Table 1. The outer-toothed clutches were fixed to the housing via an outer guide, so thermistors were inserted while the rotating inner-toothed clutches were not. The thermistor was inserted into the middle of the radial width of the clutch. The gap between the hole and the thermistor was filled with liquid metal thermal paste with thermal conductivity of 73 W/mK. Its opening was sealed with epoxy. Since the thickness of the clutch is thin enough and the thermal conductivity of steel is high, we

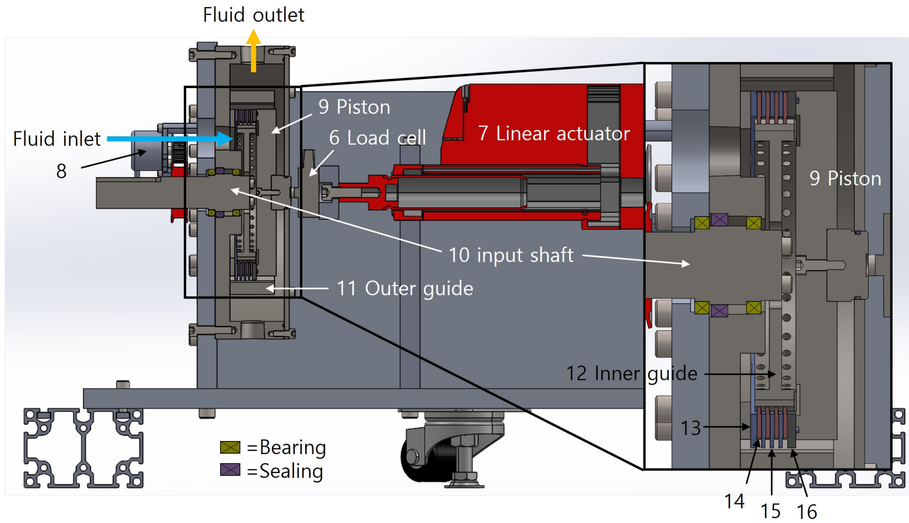

Figure 7: Cross-section of the test rig.

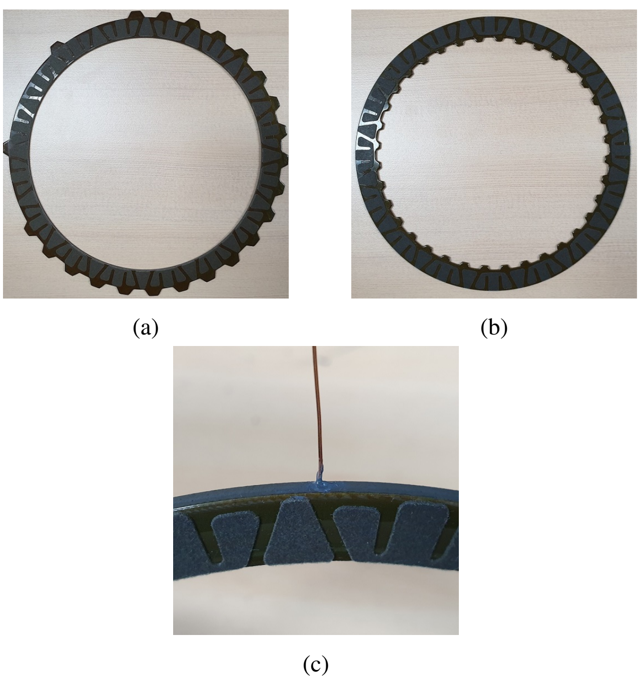

Figure 8: Single-sided clutches. (a) Outer-toothed clutch disk. (b) Inner-toothed clutch disk. (c) Thermistor implementation through side hole.

Table 1
System parameters.

Time constant of hydraulic system, τ	0.06 s
Solenoid valve gain, K	2300 Pa/mA
Piston pressure area, A_p	4981 mm^2
Friction lining area, A_f	4053 mm^2
Return spring force, F_s	593.3 N
Number of clutches, N_c	8
Generalized thermal conductivity by convection, k_1	122.2 W/K
Generalized thermal conductivity by conduction, k_2	39.94 W/K
Clutch effective radius, R_{eff}	0.07758 m
Clutch outer radius, R_o	0.08315 m
Clutch inner radius, R_i	0.07174 m
Separator thickness	1.67 mm
Friction lining thickness	0.40 mm
Young's modulus for friction lining, E	10×10^6 Pa
Asperity tip radius, β	5×10^{-4} m
RMS roughness, σ	6×10^{-6} m
Friction coefficient parameter 1, μ_1	0.1164
Friction coefficient parameter 2, μ_2	0.09562
Friction coefficient parameter 3, μ_3	0.5205
Stribeck speed, v_s	0.02424 m/s
Temperature normalization parameter 1, θ_1	40 °C
Temperature normalization parameter 2, θ_2	70 °C
Dynamic viscosity parameter 1, μ_{v1}	150.2 mPa·s
Dynamic viscosity parameter 2, μ_{v2}	-0.07838 K^{-1}
Dynamic viscosity parameter 3, μ_{v3}	58.15 mPa·s
Dynamic viscosity parameter 4, μ_{v4}	-0.02184 K^{-1}

assumed that the thermistor measures the temperature of the friction surface. Its uncertainty is 1 percent.

Clutch torque is significantly affected by the friction surface temperature, which constantly changes and usually rises during slip. In Coulomb friction coefficient modeling, the temperature of the surface is the major variable. Only after compensating for temperature effects could the influence of other variables such as slip speed and pressure be analyzed. Without considering temperature, it may show a different torque response despite the other conditions being the same. For a simple example, when the clutch slip speed is alternately a positive ramp and a negative ramp where constant pressure is applied, the transmitted torque may be different even at the same slip speed because the temperature keeps changing. In the end, the relationship between slip speed and torque may have a hysteresis characteristic or is a path function, but it is the result of friction surface temperature

Table 2
Experimental parameters.

Applied normal force		Initial slip speed		Loading period	Initial temperature
N	(kPa)	rpm	(m/s)	sec	°C
903.0	(222.8)	100	(0.8124)	5	10
1076	(265.4)	200	(1.625)	10	20
1350	(333.1)	300	(2.437)		...
1613	(397.9)				90
					100

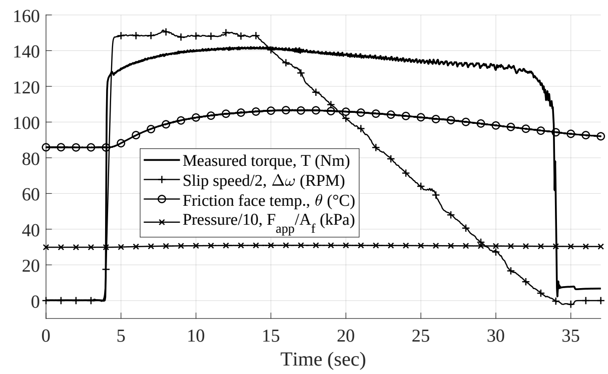

Figure 9: Experimental recordings for parameter identification.

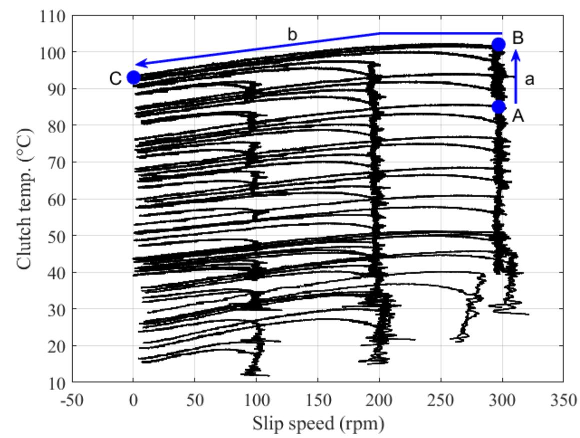

Figure 10: Clutch temperature vs. slip speed with load equal to 903.0 N during experiments.

fluctuation. Mäki et al. [20], a study on a brass lining, also emphasized the importance of temperature compensation.

The temperature of the friction surface, rather than the oil reservoir temperature, is a variable in the Coulomb friction coefficient. In this study, the temperature of the friction surface could be measured with the thermistor inserted into the clutch separator plates, which enabled more precise modeling.

3.2. Experimental data

We performed a total of 184 experimental sets of all the combinations shown in Table 2. As the temperature decreases, the magnitude of the viscous friction increases exponentially. To prevent potential surpassing of the motor torque capacity due to this increase, only a pressing force of 903 N was utilized for initial temperatures of 30 °C or lower. Specifically, initial slip speeds of 100 rpm and 200 rpm were tested at an initial temperature of 10 °C. Throughout all experiments, the oil flow rate was consistently maintained at 10 L/min.

Fig. 9 illustrates the data from a single experiment. During the experiment, the pressing force remained constant from the start to the end of rotation to uphold a steady-state fluid film thickness. The desired slip speed rapidly increased to 300 rpm from zero, held for 10 seconds, and then uniformly decreased over the next 20 seconds. The motor current was switched off when the rotation speed reached zero or less.

In Fig. 9, the period from 4 seconds to 14 seconds, where the rotation speed is kept constant, represents a loading period. This phase aims to introduce variations in the clutch surface temperature while keeping other variables constant, allowing for an analysis of individual torque influences. Following this, the clutch surface temperature depends on the balance between frictional heat generation and heat dissipation. Across all experiments, the ramp-down period remained constant at 20 seconds. The specific parameters for the experiment in Fig. 9 are a pressure of 333.1 kPa, an initial slip speed of 300 rpm, a loading period of 10 seconds, and an initial temperature of 90 °C.

Fig. 10 displays records of slip speed and temperature, where the blue dots and arrows specifically highlight the experiment detailed in Fig. 9. Commencing from the initial temperature and speed (dot A), the temperature undergoes an increase (arrow a) while maintaining the rotational speed throughout the loading period. Subsequently, the rotational speed experiences a ramp-down (curved arrow b) until the final engagement (dot C).

Using (8), the Coulomb friction coefficient is calculated as:

$$\begin{aligned}\mu_f &= \frac{T - T_v}{R_{eff} N_c F_c} \\ &= \frac{T - R_{eff} N_c \mu_v(\theta) A_f v / h(F_c)}{R_{eff} N_c F_c}.\end{aligned} \tag{17}$$

T, v, F_{app} and θ are measured values from the experiment, and other constants and variables are detailed in Table 1.

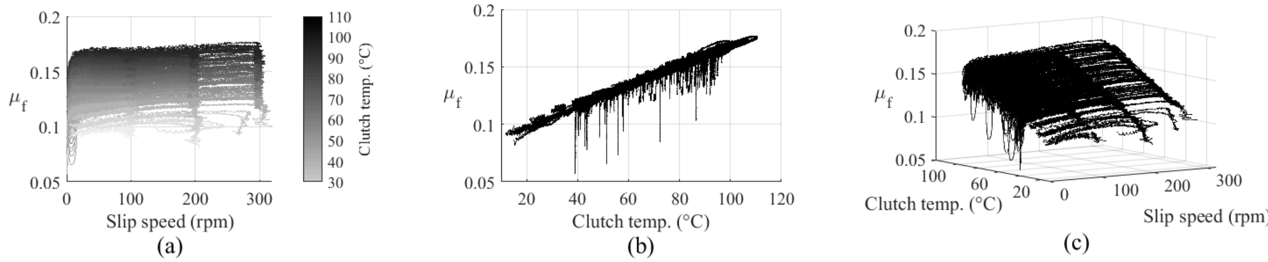

Figure 11: Experiment results. (a) μ_f to slip speed $\Delta\omega$. (b) μ_f to temperature θ. (c) 3D plot of μ_f vs. slip speed $\Delta\omega$ and temperature θ.

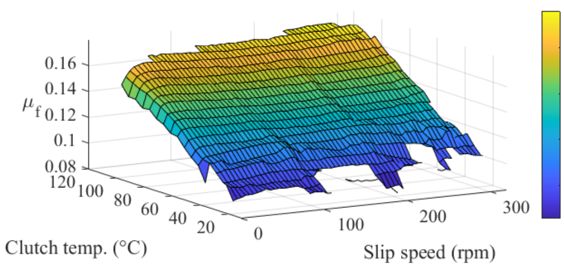

Figure 12: Calculated Coulomb friction coefficient μ_f.

Calculated results are then presented in Fig. 11 as functions of slip speed and temperature. In Fig. 11a, there may appear to be an increase in the Coulomb friction coefficient with slip speed above 20 rpm. However, this increase is attributed to temperature variation. When compared at the same temperature, the friction speed exhibits an insignificant effect on the Coulomb friction coefficient beyond 20 rpm or 0.16 m/s. This also supports the necessity for the Coulomb friction coefficient model to incorporate a term addressing temperature, especially since it maintains a flat shape after a certain speed, suggesting the appropriateness of an exponential function for frictional speed. In Fig. 11b, the temperature's effect yields a linear result within the experimental range. Notably, the normal force shows no discernible effect, aligning with the findings of [17] for brass material.

For clearer graphical representation, Fig. 12 organizes the data into a uniformly spaced grid with intervals of 5 rpm and 5 °C, creating a surface with the average value within each grid. At low frictional speeds, there is an exponential increase, while at speeds exceeding 20 rpm (0.16 m/s), the Coulomb friction coefficient shows independent result to the slip speed. Within the experimental range, the temperature's effect could be described as linear.

3.3. Coulomb friction coefficient model

Based on the experimental results, the Coulomb friction coefficient model structure was constructed as follows:

$$\mu_f(v,\theta) = \left(\mu_1 + \left(\mu_2 - \mu_1\right) e^{-v/v_s}\right) \cdot \left(1 + \mu_3 \frac{\theta - \theta_1}{\theta_2}\right). \tag{18}$$

The first part for velocity is an exponential function, and the second part for temperature is a linear function. The exponential function related to speed is a representative structure embodying the Stribeck effect in lubricated friction. Notably, the effect of temperature on the Coulomb friction coefficient demonstrates linearity, as illustrated in Fig. 11b. To account for the general operating temperature range of AT, which spans from 40 °C to 110 °C, the temperature-related terms are normalized within this range. The exponential term and the linear term exhibit a multiplicative relationship. This structural choice arises from the simultaneous expansion of the Stribeck curve with an increase in temperature, establishing a multiplicative, rather than additive, relationship between these two terms.

The physical interpretations of the parameters are as follows: μ_1 represents the Coulomb friction coefficient at 40 °C; μ_2 signifies the Coulomb friction coefficient at micro-friction speed at 40 °C; v_s denotes the Stribeck speed; μ_3 serves as the linear regression coefficient for temperature; and θ_1 and θ_2 are temperature normalization parameters. Notably, the value of $\mu_2 - \mu_1$ varies significantly depending on the type of oil, with the sign potentially differing as well. In this study, the oil used yields a negative value, indicating a descending curve for decreasing frictional speed. Contrastingly, some studies have reported positive values [10, 16, 20].

Considering speed, an exponential function was adopted. In (18), the exponential term approaches zero for slip speeds exceeding 12 rpm (0.097 m/s), which is four times the Stribeck speed. Within the experimental scope, it can be argued that the Coulomb friction coefficient remains unaffected by a friction speed surpassing this value.

The Stribeck effect occurs in a micro slip speed range (under 12 rpm and 0.097 m/s). This range is very narrow compared to the entire modeled scope, and considering that the Stribeck effect introduces nonlinearities to the model, it can be argued that its absence might actually contribute to enhancing the overall model accuracy. As the number of parameters increases, the difficulty in identification also rises. Nevertheless, despite these challenges, the modeling of this small curve is essential. In clutch engagement control, control performance is demanded to be higher as the slip speed decreases. In other words, the friction model should be most accurate just before the engagement. If the Stribeck curve is not considered in the model, the actual frictional

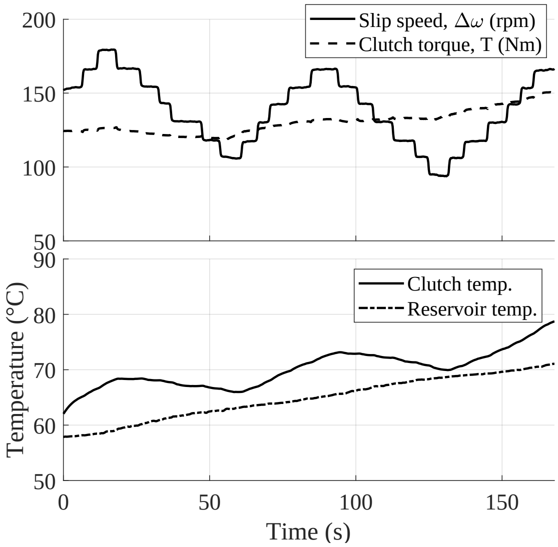

(a) Small stepwise changes in thermal energy input.

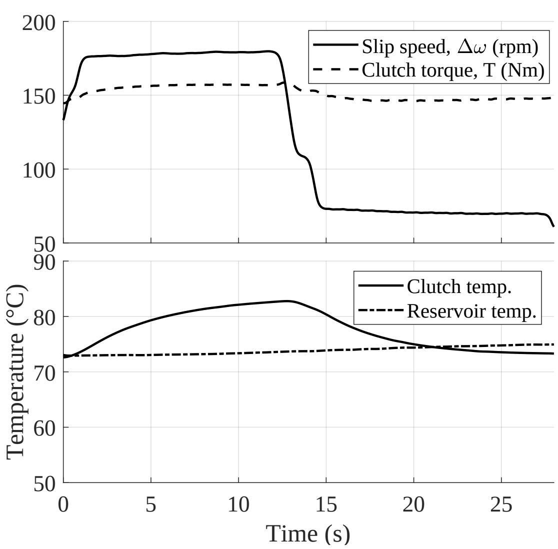

(b) Large stepwise changes in thermal energy input.

Figure 13: Thermal conductivity identification experiment.

force may occur lower than predicted by the controller. This could lead to an inability to engage at the targeted time, allowing the friction speed to rise again, and vibrations may occur. Furthermore, such vibrations could exacerbate the stick-slip problem. Therefore, the Stribeck curve is necessary in the control-oriented modeling of friction.

The coefficients were obtained by multiple linear regression on temperature and slip speed and are presented in Table 1. The coefficient of determination between the experimental data Fig. 11c and the model plane (18) is 0.9858, and root-mean-square-error (RMSE) of them is 0.002102.

3.4. Thermal conductivity identification

To identify the generalized thermal conductivities, experiments were conducted to measure the temperature of

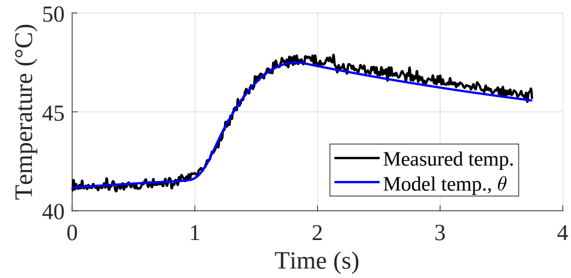

Figure 14: Temperature estimation results in clutch engagement.

each part while changing the thermal input. As shown in Fig. 13, the thermal input fluctuated by changing the rotational slip speed $\Delta\omega$. In Fig. 13a, small and frequent stepwise changes were made to the slip speed, and in Fig. 13b, a large stepwise change was made to the slip speed. To identify correct coefficients, the experiment was conducted much longer than the time it takes to engage the clutch.

Equation (1) can be modified for multiple linear regression as follows:

$$T\Delta\omega - \{(mc_p)_{lining} + (mc_p)_{separator}\}N_c\dot{\theta} = k_1(\theta - \theta_{oil}) + k_2(\theta - \theta_{housing}). \quad (19)$$

The left-hand side can be calculated from the measured values, and k_1 and k_2 can be obtained by multiple linear regression on the temperature differences.

3.5. Model verification and discussion

In order to verify the accuracy of the model, experiments were conducted to simulate the clutch engagement using the same equipment and plotted in Fig. 15. The experimental procedure was designed to simulate clutch engagement over 1 second. Starting at an initial slip speed of 750 rpm, the piston moves and compresses the clutch, creating friction and eventually engaging the clutch. A step load of 1188 N (pressure of 293.1 kPa) was used for the pressing force. The green line indicates the viscous torque calculated by (7). Equation (6), (8) and (18) were used to calculate the model torque T and Coulomb friction torque T_c, and are displayed as blue and red lines, respectively. The estimated clutch temperature was used in the calculation. In Fig. 15, the clutches contact at 0.9 seconds. Before 0.9 s, the viscous torque gradually increases as the nominal separation between the clutches narrows as the piston continues to move. A pressing force develops with the contact, thus increasing the clutch torque up to 180 Nm with increasing Coulomb friction. The increase in torque reduces the clutch slip speed and engages the clutch in 1.9 s.

The viscous torque is a function of the slip speed, temperature, and normal force. At the beginning of the engagement (0.9 s to 1.1 s in Fig. 15b), the slip speed is almost unchanged, but the nominal clutch separation is rapidly reduced, resulting in a significant increase in viscous torque up to 54.6 Nm. During the clutch engagement, the viscous

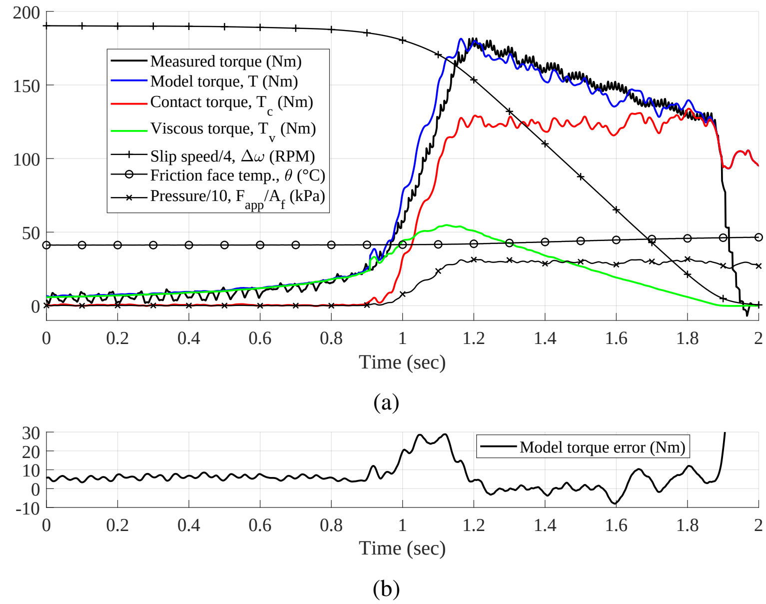

Figure 15: Experiment simulating clutch engagement for model verification (a) and its torque error plot (b).

torque decreases with the slip speed and finally converges to zero. The proposed model has a straightforward structure that can calculate the viscous torque with the pressing force (i.e., the oil pressure).

In Fig. 15b, the model torque shows a good agreement to the measurements with minor errors. Errors mainly arise from model assumption errors. Before 1.2 s, as the pressing force increases rapidly, the fluid film thickness changes significantly, i.e., the fluid film dynamics are transient-state. The maximum error occurs in this transient-state and is up to 28.9 Nm. After 1.2 s, the pressing force remains constant, the steady-state assumption is satisfied, and the error decreases to a maximum of 12 Nm. The RMSE in steady-state is 2.25 Nm, which is small enough for the model accuracy for clutch control. In experiments using different initial slip speeds of 250 rpm and 500 rpm, the RMSE in steady-state was 2.98 Nm and 3.03 Nm, respectively. The vibration of model torque is mainly due to the load cell measurement noise. Measurements fluctuate despite filtering and also affect the torque model. Therefore, if the piston pressure, which is the model input, is accurately known, the proposed method provides an accurate wet clutch friction torque.

One of the causes of error is that the average of the measured temperatures may differ from the actual average temperature of the clutch surface. Temperature measurement points were at the bottom of non-rotating outer-toothed clutches, and the temperature may not be uniform for the following reasons: the piston pushes the clutch non-uniformly; the coolant cools the clutches non-uniformly; and the value measured by the thermistor has an error with the surface temperature.

The clutch engages at 1.9 s in Fig. 15, but the motor power is still on. Because the friction model cannot express the friction force at zero velocity, there is a difference between the model and the measured torque after engaging. The reason that the measured torque drops with slight vibration after the clutch engagement is the torsional stiffness of the shaft from the inertia to the clutch.

In Fig. 14, the estimated temperature is plotted for comparison with the measured values. Temperature estimation using simplified thermal dynamics makes it possible to estimate the temperature of the clutch in real-time within a small error range and use the temperature of the clutch friction surface in the friction model.

The clutch system is a key component in altering the connectivity of the vehicle powertrain. In a vehicle, clutches are frequently disengaged and engaged while driving. Improper control at the moment of clutch engagement can diminish the lifespan of components and induce excessive jerk, thereby causing discomfort to the driver. Issues related to clutch engagement control predominantly arise from an elevation in clutch surface temperature beyond acceptable limits, and aside from solutions grounded in material or mechanical engineering, control theories also offer a viable resolution [30, 31]. A notable advantage of employing precision control methods lies in the minimal or absent need for hardware alterations. Additionally, model-based control is inherently contingent upon the accuracy of the model, exerting a direct influence on the outcomes of the control. Ultimately, the objective of the control-oriented model proposed in this paper is the enhancement of wet clutch control performance.

4. Concluding remarks

We presented a parametric analysis on the modeling of wet clutch friction, specifically examining the influences of normal force, frictional speed, and temperature. Experimental equipment and procedures for the analysis were also presented. A reduced-order friction model for control-oriented modeling was proposed and verified by experiments. The steady-state assumption on oil film dynamics enables the calculation of the clutch nominal separation and viscous friction. A wet clutch with paper-based friction lining and ATF were used in the experiments, with parameter ranges spanning from 222.8 kPa to 397.9 kPa for pressure, 10 °C to 110 °C for temperature, and 1 mm/s to 2.43 m/s for slip speed.

The following conclusions can be drawn from our study:

- The Coulomb friction coefficient varies with slip speed and surface temperature. Its relationship is exponential with slip speed and linear with friction surface temperature.
- The Coulomb friction coefficient of a wet clutch with paper-based friction lining is not significantly affected by the pressure.
- The temperature of the friction surface, rather than the oil reservoir temperature, is a major variable in the Coulomb friction coefficient. The temperature of the oil reservoir is an indirect variable.
- Assuming a steady-state condition simplifies the film thickness dynamics, and the simplified average film thickness enables the calculation of viscous torque.
- Through assumptions, a control-oriented friction modeling method and a simplified clutch torque model that could improve gear shift control performance are proposed.

Acknowledgement

This research was supported by the BK21+ program through the NRF funded by the Ministry of Education of Korea; the Technology Innovation Program (Development of innovative design for UX environment improvement and commercialization model of wheelchair electric motorization kit with enhanced portability and convenience) funded By the Ministry of Trade, Industry & Energy(MOTIE, Korea) [grant numbers 20010263]; and the National Research Foundation of Korea(NRF) grant funded by the Korea government(MSIP) [grant numbers 2020R1A2B5B01001531].

References

[1] J. J. Oh, S. B. Choi, J. Kim, Driveline modeling and estimation of individual clutch torque during gear shifts for dual clutch transmission, Mechatronics 24 (2014) 449–463.

[2] M. Holgerson, Optimizing the smoothness and temperatures of a wet clutch engagement through control of the normal force and drive torque, J. Trib. 122 (2000) 119–123.

[3] H. Khalil, Nonlinear Systems, Pearson Education, Prentice Hall, 2002. URL: https://books.google.co.kr/books?id=t_d1QgAACAAJ.

[4] S. Devasia, Should model-based inverse inputs be used as feedforward under plant uncertainty?, IEEE Transactions on Automatic Control 47 (2002) 1865–1871.

[5] C. A. Coulomb, Théorie des machines simples en ayant égard au frottement de leurs parties et à la roideur des cordages, Bachelier, 1821.

[6] E. Berger, F. Sadeghi, C. Krousgrill, Finite element modeling of engagement of rough and grooved wet clutches, Journal of Tribology 118 (1996) 137–146.

[7] M. Li, M. Khonsari, D. McCarthy, J. Lundin, Parametric analysis for a paper-based wet clutch with groove consideration, Tribology International 80 (2014) 222–233.

[8] Y. Yang, R. C. Lam, Y. F. Chen, H. Yabe, Modeling of heat transfer and fluid hydrodynamics for a multidisc wet clutch, SAE transactions (1995) 1674–1688.

[9] M. Holgerson, J. Lundberg, Engagement behaviour of a paper-based wet clutch part 1: influence of drive torque, Proceedings of the Institution of Mechanical Engineers, Part D: Journal of Automobile Engineering 213 (1999) 341–348.

[10] M. Holgerson, J. Lundberg, Engagement behaviour of a paper-based wet clutch part 2: influence of temperature, Proceedings of the Institution of Mechanical Engineers, Part D: Journal of Automobile Engineering 213 (1999) 449–455.

[11] Y. Kimura, C. Otani, Contact and wear of paper-based friction materials for oil-immersed clutches—wear model for composite materials, Tribology International 38 (2005) 943–950. Tribology International A Celebration Issue.

[12] M. Holgerson, Apparatus for measurement of engagement characteristics of a wet clutch, Wear 213 (1997) 140–147.

[13] M. Li, M. Khonsari, D. McCarthy, J. Lundin, On the wear prediction of the paper-based friction materialin a wet clutch, Wear 334 (2015) 56–66.

[14] M. Li, M. Khonsari, D. McCarthy, J. Lundin, Parametric analysis of wear factors of a wet clutch friction material with different groove patterns, Proceedings of the Institution of Mechanical Engineers, Part J: Journal of Engineering Tribology 231 (2017) 1056–1067.

[15] N. Lingesten, P. Marklund, E. Höglund, M. Lund, J. Lundin, R. Mäki, Apparatus for continuous wear measurements during wet clutch durability tests, Wear 288 (2012) 54–61.

[16] P. Marklund, R. Mäki, R. Larsson, E. Höglund, M. M. Khonsari, J. Jang, Thermal influence on torque transfer of wet clutches in limited slip differential applications, Tribology international 40 (2007) 876–884.

[17] P. Marklund, R. Larsson, Wet clutch friction characteristics obtained from simplified pin on disc test, Tribology International 41 (2008) 824–830.

[18] V. Ivanović, Z. Herold, J. Deur, M. Hancock, F. Assadian, Experimental characterization of wet clutch friction behaviors including thermal dynamics, SAE International Journal of Engines 2 (2009) 1211–1220.

[19] V. Ivanović, J. Deur, Z. Herold, M. Hancock, F. Assadian, Modelling of electromechanically actuated active differential wet-clutch dynamics, Proceedings of the Institution of Mechanical Engineers, Part D: Journal of Automobile Engineering 226 (2012) 433–456.

[20] R. Mäki, P. Nyman, R. Olsson, B. Ganemi, Measurement and characterization of anti-shudder properties in wet clutch applications, Technical Report, SAE Technical Paper, 2005.

[21] L. Yu, B. Ma, M. Chen, H. Li, C. Ma, J. Liu, Comparison of the friction and wear characteristics between copper and paper based friction materials, Materials 12 (2019).

[22] H. Cui, Q. Wang, Z. Lian, L. Li, Theoretical model and experimental research on friction and torque characteristics of hydro-viscous drive in mixed friction stage, Chinese Journal of Mechanical Engineering 32 (2019) 1–11.

[23] G. Pica, C. Cervone, A. Senatore, M. Lupo, F. Vasca, Dry dual clutch torque model with temperature and slip speed effects, Intelligent Industrial Systems 2 (2016) 133–147.

[24] B. Wu, D. Qin, J. Hu, X. Wang, Y. Wang, H. Lv, Analysis of influencing factors and changing laws on friction behavior of wet clutch, Tribology International 162 (2021) 107125.

[25] J. Deur, J. Petric, J. Asgari, D. Hrovat, Modeling of wet clutch engagement including a thorough experimental validation, SAE transactions (2005) 1013–1028.

[26] A. Myklebust, L. Eriksson, Modeling, observability, and estimation of thermal effects and aging on transmitted torque in a heavy duty

truck with a dry clutch, IEEE/ASME transactions on mechatronics 20 (2014) 61–72.
[27] N. Patir, H. S. Cheng, Application of Average Flow Model to Lubrication Between Rough Sliding Surfaces, Journal of Lubrication Technology 101 (1979) 220–229.
[28] S. Natsumeda, T. Miyoshi, Numerical simulation of engagement of paper based wet clutch facing, Journal of Tribology 116 (1994) 232–237.
[29] J. A. Greenwood, J. P. Williamson, Contact of nominally flat surfaces, Proceedings of the royal society of London. Series A. Mathematical and physical sciences 295 (1966) 300–319.
[30] B. Gao, H. Chen, H. Zhao, K. Sanada, A reduced-order nonlinear clutch pressure observer for automatic transmission, IEEE Transactions on Control Systems Technology 18 (2010) 446–453.
[31] B. Z. Gao, H. Chen, K. Sanada, Y. Hu, Design of clutch-slip controller for automatic transmission using backstepping, IEEE/ASME Transactions on Mechatronics 16 (2011) 498–508.

Seungin Shin received the B.S., the M.S. and Ph.D. degrees in mechanical engineering from Korea Advanced Institute of Science and Technology (KAIST), Deajeon, Korea, in 2017, 2018 and 2023, respectively. Since 2023, He has taken the position of Staff Engineer at Samsung Electronics. His current research interests include systems modeling, vehicle driveline control and iterative learning control.

Seibum B. Choi received the B.S. degree in mechanical engineering from Seoul National University, Seoul, South Korea, the M.S. degree in mechanical engineering from Korea Advanced Institute of Science and Technology (KAIST), Daejeon, South Korea, and the Ph.D. degree in controls from the University of California, Berkeley, Berkeley, CA, USA, in 1993. Since 2006, he has been with the Faculty of the Mechanical Engineering Department, KAIST. His research interests include fuel saving technology, vehicle dynamics and control, and application of self-energizing mechanism.